Measurement of the Σ^+ Magnetic Moment*

P. W. ALLEY, J. R. BENBROOK,† V. COOK, G. GLASS, K. GREEN,
J. F. HAGUE,‡ AND R. W. WILLIAMS
Physics Department, University of Washington, Seattle, Washington 98105
(Received 3 September 1970)

The magnetic moment of the Σ^+ hyperon has been measured to be 2.7 ± 1.0 nuclear magnetons.

I. INTRODUCTION

THERE have been several measurements of hyperon magnetic moments over the past few years.[1–10] Accurate values for these parameters will provide valuable tests for particle theories and are essential to an understanding of the structure of the hyperons. This paper reports a measurement of the Σ^+ magnetic moment, which, although it combines good statistics and high field, proves to have a precision only slightly better than that of previous determinations.[6–10] Nevertheless, we believe that it is a reliable result which provides further support for the $SU(3)$ prediction that the Σ^+ and proton have the same magnetic moment, in the absence of symmetry-breaking corrections.

The technique used in the experiment reported here is identical in concept to that used in previous hyperon magnetic moment measurements. The hyperons were produced in the reaction

$$\pi^+(1280\ \mathrm{MeV}/c)+p \rightarrow K^+ + \Sigma^+ \searrow p+\pi^0 \qquad (1)$$

and were subjected to a large (nearly) longitudinal magnetic field until they decayed via the parity-violating weak interaction. The asymmetric distribution of the decay protons relative to the Σ^+-spin direction provides a measure of the Σ^+-spin precession and therefore a measure of the Σ^+ magnetic moment.

The projected-angle distribution of the decay protons from polarized Σ^+ which are produced in a magnetic field can be written

$$f(\nu)=1+\tfrac{1}{4}\pi\alpha P\cos(\nu-\mu b),$$
$$b\equiv -\frac{em_\Sigma}{P_\Sigma m_p}\int \mathbf{B}\cdot d\mathbf{l}, \qquad (2)$$

where ν is defined in Fig. 1(a), α is the decay asymmetry parameter, P is the average Σ^+ polarization for the sample, μ is the value of the Σ^+ magnetic moment in nuclear magnetons, m_Σ, P_Σ, and e are the mass, momentum, and charge of the Σ^+, m_P is the proton mass, $\mathbf{B}$ is the value of the magnetic field, and the integral is to be taken over the flight path of the Σ^+.

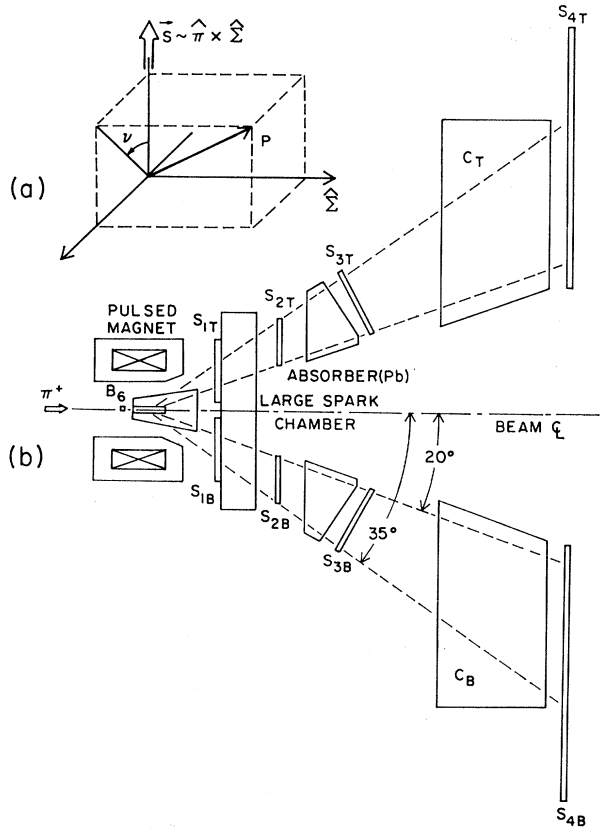

FIG. 1. (a) Coordinate frame defining projected angle and positive Σ^+-spin direction. (b) Schematic cross section of apparatus. The event trigger logic can be written ($B6$ and S represent scintillation counters) as follows:

$T=\{B6+S1T+S2T+S3T+CT(\text{delayed})+S1B$
$+(S4T \text{ and } CT \text{ in prompt anticoincidence})$; or
$B6+S1B+S2B+CB(\text{delayed})+S1T$
$+(S4T \text{ and } CB \text{ in prompt anticoincidence})\}$.

* Research support by the National Science Foundation.
† Present address: Physics Department, University of Houston, Houston, Tex. 77004.
‡ Present address: 9 Heron's Place, Marlow, Bucks, England.
[1] R. L. Cool *et al.*, Phys. Rev. **127**, 2223 (1962).
[2] W. Kernan *et al.*, Phys. Rev. **129**, 870 (1963).
[3] J. A. Anderson *et al.*, Phys. Rev. Letters **13**, 167 (1964).
[4] D. A. Hill *et al.*, Phys. Rev. Letters **15**, 85 (1965).
[5] G. Charriere *et al.*, Nuovo Cimento **46A**, 206 (1966).
[6] V. Cook *et al.*, Phys. Rev. Letters **17**, 223 (1966).
[7] C. R. Sullivan *et al.*, Phys. Rev. Letters **18**, 1163 (1967). This paper includes a reanalysis of some early data first reported by A. D. McInturff and C. E. Roos, *ibid.* **13**, 246 (1964).
[8] D. Kotelchuck *et al.*, Phys. Rev. Letters **18**, 1166 (1967).
[9] J. Combe *et al.*, Nuovo Cimento **57A**, 54 (1968).
[10] T. Mast *et al.*, Phys. Rev. Letters **20**, 1312 (1968).

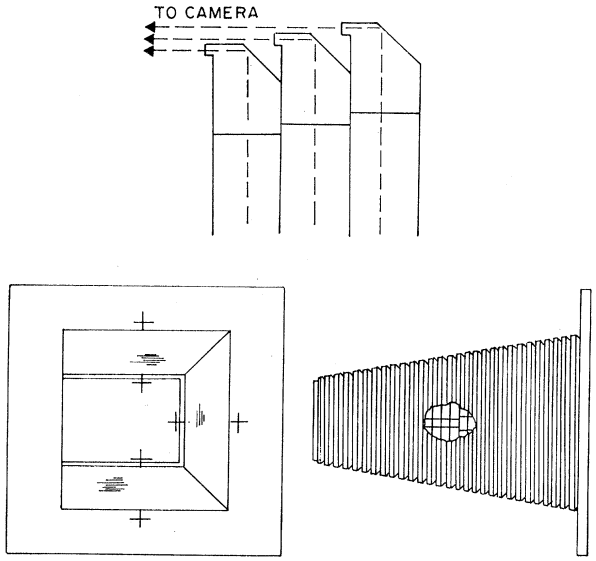

FIG. 2. Spark chamber (located inside solenoid) with cutaway view of target and Styrofoam spacers, and expanded cross section of three spark-chamber frames illustrating how light was internally reflected through 90° and emerged nearly parallel to the beam axis.

II. APPARATUS

A schematic view of the experimental apparatus is shown in Fig. 1. The main components are the following.

(a) A separated (1280 MeV/c) π^+ beam from a target in the external proton beam of the LRL Bevatron.

(b) Pulsed solenoid magnet[11]: 9.4 cm i.d., 13 cm along the axis; max field 145 kG; repetition rate 0.1 sec^{-1}.

(c) Optical spark chamber and production target located inside solenoid (Fig. 2): 30 0.5-cm gaps tapered in area to facilitate light collection along beam axis; production target, 6.3-mm-high strips of CH_2 mounted inside the first 16 spark-chamber gaps.

(d) K^+ and proton detector: Water Čerenkov counter and scintillation counters to select K^+'s of the proper momentum which stop in the water and whose decay products are detected in the upper (lower) segment with scintillation counter signal (decay proton) in the lower (upper) segment. Each of the "top" (T) and "bottom" (B) segments of the K^+ detector covered 120° of the azimuth. A picture of the detector can be gene-

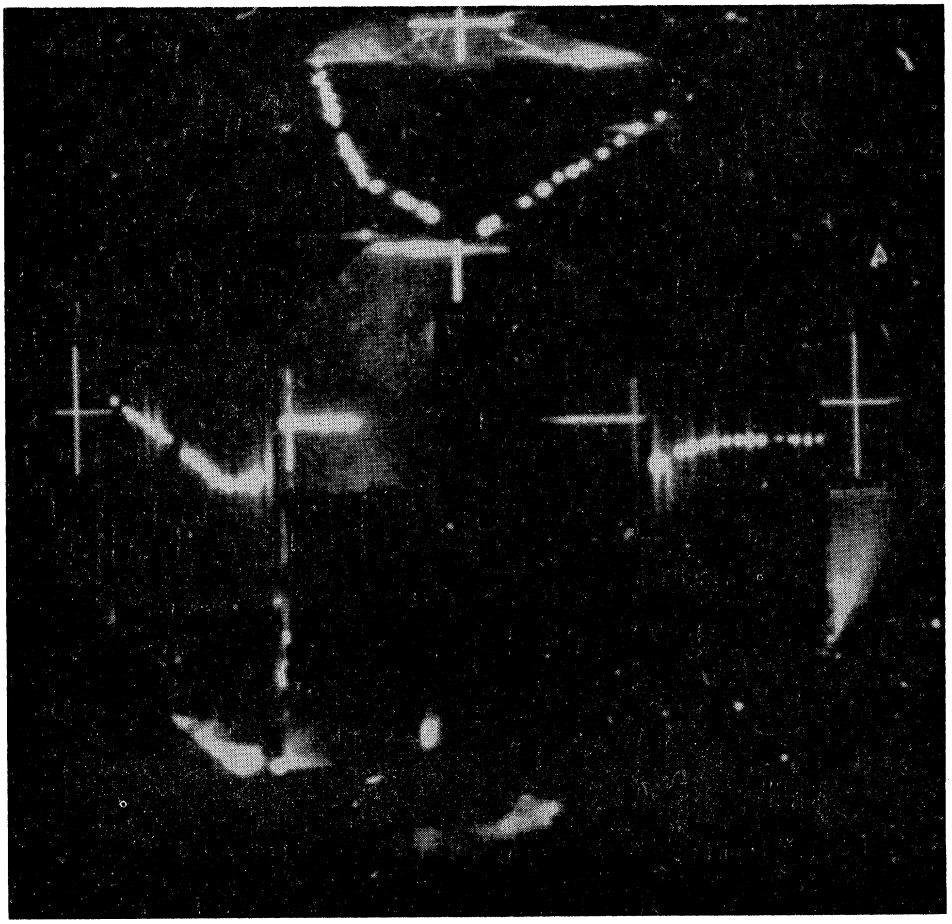

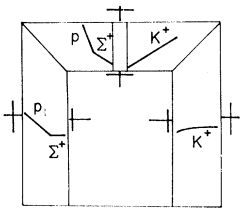

FIG. 3. Typical "selected" Σ^+ event.

[11] For a description of a similar magnet, see G. McD. Bingham *et al.*, Phys. Rev. D 1, 3010 (1970).

rated by rotating the layout shown in Fig. 1(b) about the beam axis through 60° from a vertical plane.

The spark-chamber pulsing system was triggered when the appropriate coincidence signal was produced (see Fig. 1). A rapid cycling 35-mm camera photographed the spark chamber and a digital counter which displayed the instantaneous value of the magnetic field.

III. DATA ANALYSIS

Out of 4×10^5 pictures (3.8×10^{10} incident π^+) taken during the experiment, some 9000 measurable candidates for reaction (1) were found. A typical "good event" is shown in Fig. 3. (A comparable number of

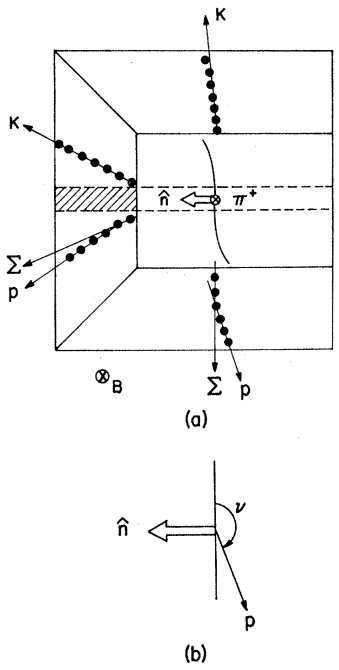

FIG. 4. (a) Drawing of a "curved-track" event which is interpreted as an event of type (1). The projection of the two tracks on a plane normal to the beam direction is shown where it is assumed that both particles are positively charged and the field is downstream (+). (b) The ν value for this event would be near $90°<\nu<270°$, i.e., in the "down" hemisphere.

"Λ events" were also found.) Between two and five points were measured on the three observed tracks in both (90° stereo) views and a minimized χ^2 was calculated on the hypothesis that these were reaction-(1)-type events. For each of these candidates, where feasible, second-degree curves were determined for each of the tracks. About 3800 events survived a reasonable set of quantitative selection requirements. Because the fit was loosely constrained, it was found necessary to make a further qualitative selection to eliminate two-body final states in which one of the tracks was sufficiently curved to simulate reaction (1). This selection was made by physicists who assigned a qualitative grade to each event. The "curved-track" events, when interpreted as events of type (1), produce a very strongly biased projected-angle distribution. This effect is illustrated in Fig. 4. Note that one expects a preponderance of curved-track events to fall in the projected-angle range $90°<\nu<270°$ for (+) field (as illustrated in Fig. 4). It is clear that for the (−) field direction the effect will produce an excess in the angular region $-90°<\nu<+90°$. This effect should result in a large positive αP value for the (−) field events and negative αP for (+) field events. The αP values for these events which were classified as "curved track," and thus eliminated from the final sample, are shown in Table I. The αP values for the selected "good events" are given in Table II. We note that there is a difference between the (+) and (−) field values, which indicates that there are still curved-track events which the selection process has not eliminated. Since the average precession angle is small (17°) compared with 180°, the error in μ_Σ cancels when the two sets of data are analyzed together, provided the quantity (number of events)$\times\langle\int\mathbf{B}\cdot d\mathbf{l}\rangle$ is the same for both field signs. The error due to imperfect cancellation is estimated to be $<0.1\mu_N$. This estimate is supported by the insensitivity of μ_Σ to the bias function (see Sec. V).

TABLE I. Asymmetry parameters for the data rejected as "curved-track" events.

	No. of events	αP
(+) field	774	-1.19 ± 0.07
(−) field	674	$+0.90\pm0.08$
Combined	1448	-0.22 ± 0.05

The Σ^+ produced off free protons in reaction (1) at 1280 MeV/c have a laboratory angular distribution which is sharply peaked near the maximum angle of 22°. A histogram showing the distribution of $\theta_\Sigma^{\text{lab}}$ for the selected events is shown in Fig. 5. The width of the peak is consistent with measurement errors $[\sigma(\theta_\Sigma^{\text{lab}})\sim\pm2°]$.

The decay times in the c.m. system for the K^+ and Σ^+ detected in this experiment are shown in Fig. 6. The K^+ decay time [Fig. 6(a)] was deduced from the electronically measured time interval between the K^+-telescope prompt signal, indicating that a charged

TABLE II. Results of maximum-likelihood fits to the data for the three magnetic field conditions.

Mag. field	No. of events	αP	μ_Σ
(+)	516	-0.603 ± 0.044	1.40 ± 1.22
(0)	822	-0.560 ± 0.058[a]	
(−)	439	-0.501 ± 0.047	4.35 ± 1.11
All data	1777	-0.558 ± 0.039	2.67 ± 0.97

Coeff. of $\epsilon(\nu)$ determined from zero-field data.

B_1	A_2	B_3	A_4
0.555 ± 0.045	0.025 ± 0.049	0.002 ± 0.048	-0.033 ± 0.047

[a] This uncertainty is large relative to the (+) and (−) field results because the (0) field data were also used to determine the $\epsilon(\nu)$ coefficients.

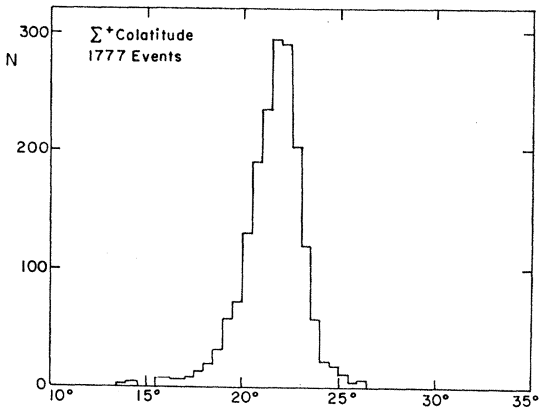

FIG. 5. Distribution of Σ^+ colatitude for selected events.

particle stopped in the water Čerenkov counter, and the Čerenkov signal which is interpreted as the decay muon or pion. The K^+ mean life determined from this distribution is in good agreement with the known K^+ lifetime. The Σ^+ decay time [Fig. 6(b)] is determined from the fitted kinematic quantities for the Σ^+. This distribution is consistent with the known Σ^+ lifetime and the experimental limits imposed by detector geometry and scanning efficiency.

The final sample consisted of a total of 1777 events: 822 with no magnetic field [(0) field], 516 with positive field [$\mathbf{B}\cdot\mathbf{p}_\pi>0$, (+) field], and 439 with negative field [$\mathbf{B}\cdot\mathbf{p}_\pi<0$, (−) field].

The observed projected-angle distribution differs from the theoretical distribution [Eq. (2)] because the detection apparatus does not have equal efficiency for detecting events at all projected angles. We write

$$f_{\text{expt}}(\nu)=\epsilon(\nu)f(\nu)\,, \tag{3}$$

where the function $\epsilon(\nu)$ is the average event-detection efficiency. This correction to the basic physical distribution is due mainly to the effect of the spark-chamber optics on the observed angle between Σ and proton. The result is a detection bias which appears in the projected-angle distribution for the data [Fig. 7(a)] as a pronounced depression in the angular region 180°–360° relative to the angular region 0°–180° ("left-right bias"). In principle, such a bias will not significantly influence the result for μ_Σ if the direction of the magnetic field is reversed during the experiment. However, it does lead to a somewhat larger statistical error on the final result for μ_Σ. A Fourier expansion for $\epsilon(\nu)$ was used in the maximum-likelihood analysis,

$$\epsilon(\nu)=\frac{1+B_1\sin\nu+A_2\cos2\nu+B_3\sin3\nu+A_4\cos4\nu}{1+\frac{1}{8}\pi\alpha PB_1\sin\mu b}. \tag{4}$$

Symmetry considerations indicate that the coefficients

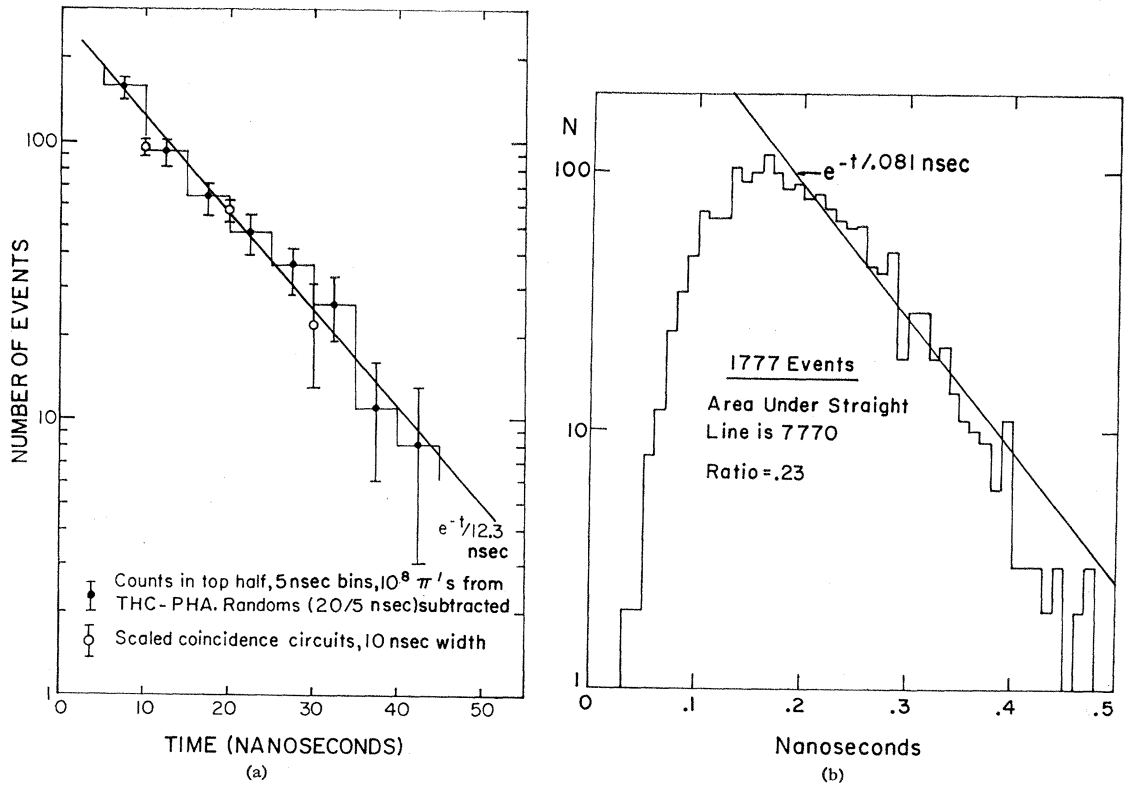

FIG. 6. (a) Distribution of measured K^+ decay times. (b) Distribution of calculated Σ^+ decay times for selected events.

of $\sin 2n\nu$ and $\cos(2n+1)\nu$ should vanish. Terms beyond $\cos 4\nu$ had negligible coefficients.

The projected-angle distributions for three different magnetic field conditions are shown in Fig. 7. The best-fit parameters (μ, α, P, B_1, A_2, B_3, and A_4), found by maximum likelihood, are given in Table II. Since the function $\epsilon(\nu)$ is expected to take account only of field-independent detection biases, we determine B_1, A_2, B_3, and A_4 from the "zero-field" data and treat them as known parameters in the "field-on" data analysis.

IV. SOURCES OF ERROR

Results of tests of the data made to determine the effects of detection biases, and calculations (or estimates) of systematic errors are summarized in the following paragraph. Some of the estimates are not precise (we have attempted to present realistic upper limits in these cases); however, a more detailed examination is not warranted by the large uncertainty in the final result. A limit on the probable error in μ_Σ is given in brackets $\{\Delta\mu<\}$ for each effect discussed. The error quoted in the result is determined in the maximum-likelihood analysis. This presumably includes all statistical errors. Systematic errors do not add significantly to the quoted error.

(i) Measuring accuracy. Uncertainties in the measured space angles ($\lesssim 2°$) lead to an uncertainty $\Delta\nu\sim 10°$ (this was found by analyzing events measured twice by different scanners). $\{\Delta\mu<10\%\}$.

(ii) Thomas precession. The average precession angle in space is $\sim 2°$–$3°$. In the projected-angle distribution this is a very small effect. $\{\Delta\mu<5\%\}$.

(iii) Measurement of $\int \mathbf{B}\cdot d\mathbf{l}$. The uncertainty in the magnetic field determination was $\pm 3\%$, and the uncertainty in $\int \mathbf{B}\cdot d\mathbf{l}$, arising mainly from uncertainty in the path length of the Σ, for each event was less than 15%. $\{\Delta\mu\lesssim 15\%\}$.

(iv) π^+-n contamination. A fraction of the π^+ from the $\pi^+ n$ decay mode of the Σ^+ could pass through the proton detectors and provide the required trigger. These events would tend to reduce the observed polarization of our sample. Phase-space limits these events to less than 15% and rejection because of reduced ionization in the spark chamber further reduces the estimated contamination to 10% of our sample. $\{\Delta\mu<1\%\}$.

(v) Minimum detectable $\theta_{\Sigma p}{}^{\rm lab}$. A detection "cutoff" on the angle between the Σ and the proton in the laboratory produces an asymmetric cutoff in the c.m. system, and therefore an "up-down" bias which can affect the value of the polarization and the magnetic moment determined from the data. A given minimum laboratory angle $\theta_{\Sigma p}{}^{\rm lab}$ produces c.m.-system cutoffs β_1 and β_2. An analysis of the effect of such cutoffs, on the projected-angle distribution (2), shows that (2) becomes

$$f(\nu)=C[1+A\times\tfrac{1}{4}\pi\alpha P\cos(\nu-\mu b)], \qquad (5)$$

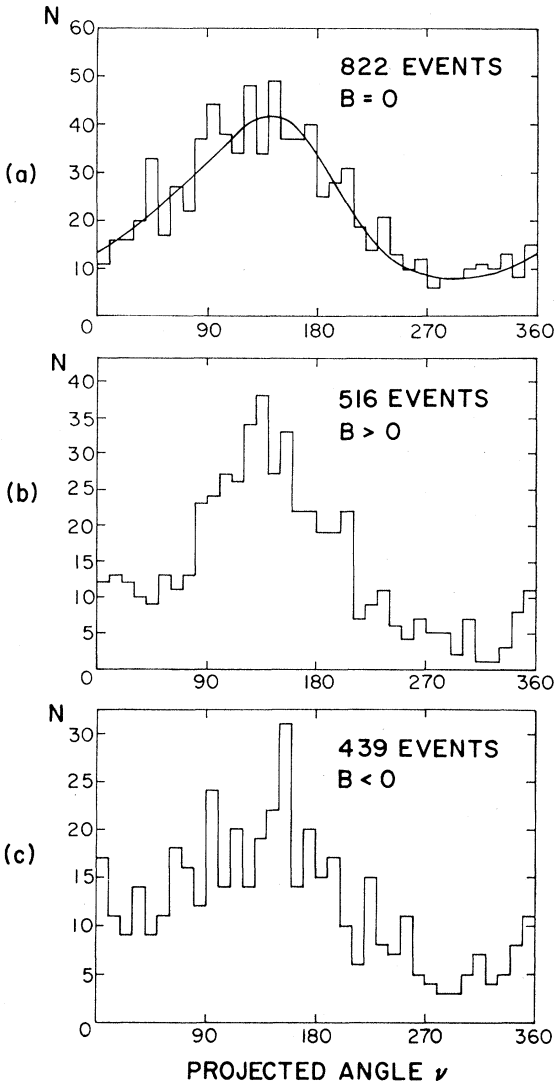

FIG. 7. Projected angle distributions of protons for (a) (0) field, (b) (+) field, and (c) (−) field data. The smooth curve in (a) is Eq. (2) evaluated with the best-fit values of the parameters.

where

$$A=\frac{(2/\pi)\sin\rho\,[(\beta_2-\beta_1)-\tfrac{1}{2}(\sin^2\beta_2-\sin^2\beta_1)]}{\cos\beta_1-\cos\beta_2-\tfrac{1}{4}\alpha P\cos\rho\,(\cos^2\beta_2-\cos^2\beta_1)} \qquad (6)$$

and ρ is the angle between the Σ-spin direction and the Σ momentum at the Σ decay point. In this experiment $\langle 1-\sin\rho\rangle\approx 0.006$, which justifies setting $\rho=90°$ in the above expression for A. Some values for A resulting

TABLE III. Calculated values for the quantity A [Eq. (6)] defined in the text for some assumed values for $\theta_{\Sigma p}{}^{\rm lab}$(min).

$\theta_{\Sigma p}{}^{\rm lab}$(min)	β_1	β_2	A
3°	15°	173°	1.021
5°	25°	167°	1.040
10°	50°	155°	1.122

TABLE IV. Summary of measurements of μ_Σ to date.

B direction[a]	B_{rms} (kG)	Technique; reaction	No. of events	$\langle\theta\rangle$[b]	αP	μ_Σ (μ_N)	Ref.
(±), (0)	80	Spark ch. $\pi^+p\to K^+\Sigma^+$	235	10°	−0.69±0.07	1.5±1.1	6
(±)	117	Emulsion $\gamma p\to K^0\Sigma^+$	51	32°	0.85±0.25	3.0±1.2	7
(±)	150	Emulsion $K^-p\to\pi^-\Sigma^+$	52	36°	−0.69±0.15	3.5±1.5	8
(±)	165	Emulsion $\pi^+p\to K^+\Sigma^+$	69	(44°)[c]	−0.70±0.34	3.5±1.2	9
d	18.7	Bubble ch. $K^-p\to\pi^-\Sigma^+$	39 000	1.46°		2.1±1.0	10
(±), (0)	100	Spark ch. $\pi^+p\to K^+\Sigma^+$	955	17°	−0.56±0.04	2.7±1.0	Present expt.
Weighted average						2.6±0.5	

[a] (±) means that two field directions were used, parallel and antiparallel to the beam direction. (0) means that data were taken with the magnetic field turned off.
[b] Average precession angle observed in the experiment.
[c] Estimated by present authors, not quoted in reference.
[d] Magnetic field was normal to incident beam direction. Only one field direction was used.

from some assumed minimum detection angles are given in Table III. The event detection efficiency in this experiment did not vary appreciably for $\theta_{\Sigma p}{}^{\rm lab}\gtrsim 10°$. Between 10° and 5° it begins to decrease and it falls rapidly for $\theta_{\Sigma p}{}^{\rm lab}<5°$. Even if we take $\theta_{\Sigma p}{}^{\rm lab}({\rm min})\approx 10°$, the effect produces a 12% change in the apparent αP value. Because αP and μ are nearly orthogonal parameters in the likelihood fit (they would be for an unbiased sample), the effect of this cutoff on the magnetic moment determination is negligible. $\{\Delta\mu<1\%\}$.

(vi) Counter detection symmetry. Although the over-all detection efficiency varied with projected proton angle, there is considerable evidence that this was caused almost entirely by the spark-chamber detection bias. For example, events triggered by the lower and upper segments of the K^+ and the proton detector yielded the same values for αP, and the K^+ azimuthal distributions were symmetric about the vertical for each half of the detector array. $\{\Delta\mu<4\%\}$.

V. RESULTS AND COMPARISON WITH OTHER DATA

The result of our experiment, using the zero-field data to determine the efficiency function, is $\mu_\Sigma=2.67\pm0.97\mu_N$. Since the bias effects should cancel out, to good approximation, when data with opposite field directions are combined, we expect that this result should not be greatly changed by setting the efficiency function equal to 1. Indeed we find that μ_Σ is changed by less than 1% when this is done. This result, and the tests listed above, give us confidence that we have treated our systematic errors correctly.

A summary of the published measurements of μ_Σ, and a weighted average, is given in Table IV.

ACKNOWLEDGMENTS

We thank the LRL director and staff for their hospitality and we are grateful for the assistance rendered us by the Bevatron crew under W. D. Hartsough during the course of this experiment.

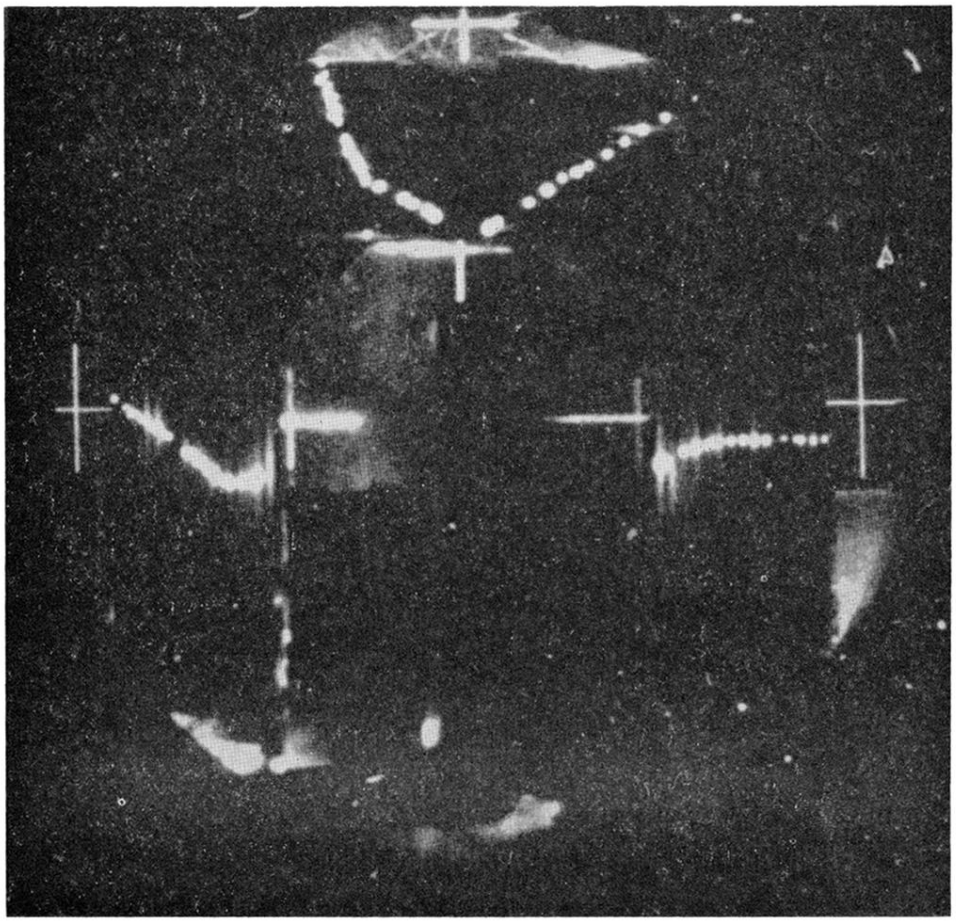

FIG. 3. Typical "selected" Σ^+ event.